ELSEVIER

Contents lists available at ScienceDirect

e-Prime - Advances in Electrical Engineering, Electronics and Energy

journal homepage: www.elsevier.com/locate/prime



Studies of corrugated antipodal vivaldi wideband antenna with notched band and rectenna integration

Nurhayati Nurhayati ^{a,*}, Mohammad Iyo Agus Setyono ^a, Ahmed J.A. Al-Gburi ^{b,*}, Lilik Anifah ^a, Lusia Rakhmawati ^a, Fitri Adi Iskandarianto ^c, Usman Ali ^d

ARTICLE INFO

Keywords: Antipodal vivaldi antenna (AVA) Rectangular spiral slot (RSS) Energy Harvesting Notched-Band Rectenna

ABSTRACT

A wideband rectenna based on a Corrugated Antipodal Vivaldi Antenna (AVA) with a notched band is proposed for energy harvesting applications. The antenna performance is studied parametrically by varying the corrugated and rectangular spiral slot (RSS) structures and also by integrating the antenna with a rectenna for energy harvesting applications. The AVA rectenna achieves an S₁₁ of less than -10 dB from 2.38 GHz to beyond 20 GHz. An AVA with two corrugations at the lower position of the radiator increases the bandwidth by 300 MHz compared to an AVA without corrugation. At 2 GHz, AVAs with three and four corrugations exhibit a directivity of 5.73 dBi, compared to 2.9 dBi for an AVA without corrugation. Increasing the corrugation depth enhances the gain, ranging from 3.05 dBi to 9 dBi. The notched band shifts to lower frequencies as the spiral strip slot lengthens, so we can set the desired notched band by adjusting the length and position of the RSS. Furthermore, Integration of a rectangular spiral slot (RSS) enables tunable notched bands, providing flexibility to reject interference from unwanted frequency ranges. The agreement between simulation and measurement confirms that the proposed AVA rectenna is also a strong candidate for wideband energy harvesting applications.

1. Introduction

Information and communication technology systems are expected to become increasingly commonplace and abundant in our surroundings due to ongoing technological advancements. Recent developments in telecommunications and radar technology include RFID, WiMAX communications [1], Bluetooth, LTE, Wi-Fi [2], vital sign monitoring [3], 5 G [4], V2X communications [5], and advancements in radar technology.

As is well known, Internet of Things (IoT) devices can be utilized across various fields, including logistics, security, energy, healthcare, and agriculture. These devices require a low-cost network, can be deployed indoors, and are often used in large quantities for identification and localization purpose [6]. IoT technology ultimately aims to wirelessly connect devices such as sensors, transmitters, receivers, and other components. With continued technological advancements, it is anticipated that billions of IoT devices will exist in the future. This growing demand directly impacts the need for energy sources, such as

batteries, which must be constantly charged or replaced, necessitating the development of self-powered systems to sustain these devices.

Rectennas are environmentally beneficial devices that enable the recycling of radio wave energy by harvesting radio frequency (RF) energy. A rectenna consists of an antenna and an RF rectifier circuit [7]. One of the key challenges in electromagnetic wave energy harvesting technology is developing sufficient power density to support self-powered devices [8].

Technological advancements have also led to the development of wireless devices capable of performing Radio Frequency Energy Harvesting (RFEH). Recently, the proliferation of wireless connections for various applications has raised concerns regarding wireless power transmission. An environment with abundant electromagnetic waves can be utilized for energy harvesting at frequencies ranging from 0.7 to 4 GHz, covering 2 G, 3 G, 4 G, 5 G, and Wi-Fi bands. However, applying energy harvesting to low-power devices remains challenging due to the need for extended battery life and the high cost of battery replacement

E-mail addresses: nurhayati@unesa.ac.id (N. Nurhayati), ahmedjamal@utem.edu.my, ahmedjamal@ieee.org (A.J.A. Al-Gburi).

^a Department of Electrical Engineering, Universitas Negeri Surabaya, Surabaya 60231, Indonesia

^b Center for Telecommunication Research & Innovation (CeTRI), Fakulti Teknologi Dan Kejuruteraan Elektronik Dan Komputer (FTKEK), Universiti Teknikal Malaysia Melaka (UTeM), Jalan Hang Tuah Jaya, 76100, Melaka, Durian Tunggal, Malaysia

^c Department of Instrumentation Engineering, Institut Teknologi Sepuluh Nopember, Surabaya 60111, Indonesia

^d Department of Telecommunication Engineering, University of Engineering and Technology, Mardan 23200, Pakistan

^{*} Corresponding authors.

[9]

Antennas and RF rectifiers play a crucial role in energy harvesting systems, as they determine the efficiency of converting ambient RF energy into usable electrical power. Research on energy harvesting antennas has been conducted by several researchers using multiband [10-13] and wideband frequencies [14-17]. One of the antennas that can work in wideband frequencies is the Vivaldi antenna. Numerous studies have been undertaken on the Vivaldi antenna to enhance bandwidth and augment gain. The Coplanar Vivaldi antenna with a rectangular corrugated shape has a size of 280 \times 170 mm and can work at a frequency of 0.32 -0.95 GHz [18]. Research on the Coplanar Vivaldi antenna with rectangular corrugated antennas has also been carried out [19] for microwave imaging applications that can work at frequencies of 1.96 - 8.61 GHz with a size of 50 \times 62 mm. Flexible rectangular corrugated Vivaldi antenna has been designed [20] for through wall radar applications with a size of 58.9×46 mm and can work in 3 frequency bands, namely 2.56-4.03 GHz, 5.03 - 5.92 GHz and 7.2 - 7.5 GHz. Studies on Vivaldi antennas including various corrugated edge constructions have been conducted to evaluate the impact of corrugation on mutual coupling performance, operating throughout the frequency range of 0.5 to 4.5 GHz [21]. Several corrugated structures have been carried out by several researchers to increase the bandwidth and gain of the Vivaldi antenna, but the resulting bandwidth is still limited.

The antenna is a crucial component of energy harvesting. It receives electromagnetic waves, while the rectifier converts the RF signal into DC form, and the matching network circuit connects the antenna to the rectifier [22]. Research on rectennas has been conducted using a Wilkinson power divider to achieve circular polarization with a rectangular patch antenna operating at frequencies of 1.8-3.15 GHz, 5.45 GHz, and 5.8 GHz [23]. A rectenna utilizing a coplanar Vivaldi antenna for energy harvesting at 2.4 GHz and 5.8 GHz has been studied in [24], producing a voltage of 1.8 V or 2.14 $\mu W/cm^2$ at 2.4 GHz and 5.8 GHz. Although this design is intended for energy harvesting applications, it has a limited bandwidth and only supports dual-band frequencies. Research on a rectangular corrugated AVA operating from 0.8 to 4.24 GHz has been discussed in [25]. However, this design has a large size ($230 \times 230 \text{ mm}^2$) with a corrugated box shape and has not yet been applied for energy harvesting measurements. In contrast, the antenna we propose features an expanded bandwidth and employs exponential corrugation. We have utilized it for energy harvesting applications and incorporated an additional structure, specifically a rectangular spiral strip slot, to enable frequency notching at multiple points. The application of Vivaldi antennas for energy harvesting remains limited, despite the fact that future energy harvesting technologies could be beneficial for various applications. A rectenna with a fractal Koch structure for energy harvesting at 1.5-2.65 GHz has been studied in [11]. Additionally, a spiral-shaped antenna capable of operating at UHF and UWB frequencies (3.1-4.8 GHz) as well as at 868 MHz has been investigated in [6]. Research on a UHF rectenna with circular right/left-hand polarization operating between 0.7 and 1 GHz, with a compact size of $164 \times 37 \text{ mm}^2$, has also been conducted for energy harvesting applications [26].

Various antenna designs have been explored for energy harvesting, but many lack wideband capabilities. Research has been conducted on wideband monopole antennas with an Split Ring Resonator (SRR) structure operating from 2 to 10 GHz, which include a notched band at 2.5–3.5 GHz [27]. A rectenna design utilizing a rectangular patch operating at 2.4 GHz has demonstrated an efficiency of 78.53 % [28]. A rectangular slot antenna operating from 1.7 to 2.7 GHz has achieved an efficiency of 40 % [29]. A dipole rectenna operating at 1.7–3 GHz has produced a power density of 7.6 μ W/cm². Furthermore, research on flexible materials for energy harvesting at 2.45 GHz has been explored in [29], demonstrating operation in the ISM band. By placing the rectenna 10 cm from a router, a voltage of 0.51 V was achieved. Additionally, a study on a rectenna operating in dual-frequency bands (2.4 GHz and 5.8 GHz) achieved efficiencies of 65.7 % and 62.4 %, respectively [30].

Rectenna research conducted so far has primarily focused on specific frequency. However, the demand for transmitting large amounts of data has significantly increased [31]. Wideband antennas can theoretically capture more energy from radio waves than narrowband antennas or circuits. This is because wideband antennas can harvest electromagnetic waves over a broad range of frequencies. A wideband antenna can gather energy from various signal sources across a larger spectrum, including TV, Wi-Fi, and radio transmissions. The potential energy received increases with the number of frequencies captured. In contrast, narrowband antennas focus on one or a few specific frequencies, limiting the amount of received energy. The criteria for a wideband antenna is if the antenna has an impedance bandwidth of more than 20 %. Vivaldi antenna can work at a very wide frequency, but for energy harvesting applications, a rectenna is needed that is adjusted to the antenna's working frequency. So by providing RSS, a notched frequency band will be formed so that the desired frequency can be notched according to the existing rectifier circuit. Therefore, developing a multiband or broadband rectenna capable of harvesting ambient RF energy from multiple frequency bands simultaneously is essential, though challenging.

Since ambient electromagnetic waves typically exhibit random polarization and varying angles of incidence, antennas designed for RF energy harvesting must possess omnidirectional radiation patterns and operate over a wide frequency range. Configurable UWB antennas with integrated energy harvesting capabilities are particularly attractive for applications such as the Internet of Things (IoT), where frequent battery replacements are impractical. Future research into battery-free antennas integrated with energy harvesting holds great promise for various intelligent and reconfigurable RF applications [32].

Research on reconfigurable antennas has demonstrated promising results. In [33], a reconfigurable approach was used to create five notched frequency bands utilizing S-shaped strips and spiral strip structures. Similarly, research on trapezoidal monopole antennas with notched bands incorporating l-shaped strips has been conducted in [34]. Research on monopole antennas using C and H slots and pin diodes to create 3 notched frequency bands has also been done in [35]. Additionally, studies on reconfigurable Vivaldi antennas have been performed in [36] and [37] where complementary split-ring resonator (CSRR) structures were implemented in coplanar Vivaldi antennas. However, these studies applied reconfigurable techniques only to monopole and coplanar Vivaldi antennas, while our research focuses on applying the reconfigurable technique to antipodal Vivaldi antennas, a topic with limited prior discussion. Typically, reconfigurable techniques involve external electronic components, requiring high accuracy. The use of reconfigurable techniques is crucial for energy harvesting antennas, as they must adapt based on the type of signal they are designed to capture.

From the discussion above, it is evident that a wideband antenna is necessary for effective radio wave energy harvesting. In this research, we focus on antipodal Vivaldi antennas capable of operating across wideband frequencies and making key contributions in this domain:

- Design a compact Corrugated Antipodal Vivaldi Antenna (AVA) that operates across a wideband frequency range from 2.38 GHz to beyond 20 GHz and supports multiband operation.
- Develop an exponential corrugated AVA structure and analyze the effect of the number and position of corrugations on the antenna'S₁₁ performance, directivity, and bandwidth enhancement.
- Optimize the shape and placement of the rectangular spiral slot (RSS) structure to generate and control notched frequency bands.
- Fabricate and measure the proposed antennas, demonstrating their suitability for wideband energy harvesting applications.

2. Antenna design

The Antipodal Vivaldi Antenna (AVA) designed in this study consists

of a copper patch with a thickness of 0.035 mm and an FR4 substrate with a relative permittivity of 4.3 and a thickness of 1.6 mm, as shown in Fig. 1. FR4 material is easy to obtain and has a relatively cheap price and is good for low and medium frequencies. However, at high frequencies, FR4 experiences increased dielectric losses. This means that some signal energy will be lost as heat, which can affect circuit performance at high frequencies.

The antenna structure is designed with a slanted tapered slot, which follows the mathematical formulation provided in Eq. (1) [31]:

$$y = C_1 e^{Rx} + C_2, C_1 = \frac{y_2 - y_1}{e^{Rx_2} - e^{Rx_1}}, C_2 = \frac{y_1 e^{Rx_2} - y_2 e^{Rx_1}}{e^{Rx_2} - e^{Rx_1}}$$
(1)

The AVA features a tapered slot design that enhances its wideband performance. The radiating patch (yellow region) and ground plane (red region) are structured to optimize impedance matching and radiation characteristics. The antenna includes an exponential corrugation structure, strategically positioned to improve directivity and enhance energy harvesting capabilities. Additionally, a spiral slot structure is incorporated within the antenna to enable frequency notching, allowing for selective band rejection.

The design and performance of the antenna were analyzed and optimized using CST Studio Suite. The software was used to simulate key parameters such as S11 performance, radiation patterns, gain, and directivity, ensuring the antenna meets the requirements for wideband energy harvesting applications.

The equation governing the slope of the tapered slot, denoted by y, depends on the constants C_1 and C_2 . These constants are determined by the initial position coordinates (X_1, Y_1) and final position coordinates (X_2, Y_2) , along with the opening rate constant R. To evaluate the return loss and directivity performance, a parametric study was conducted by varying the number and placement of corrugations on the antenna. Fig. 1 and Table 1 illustrate the antenna's dimensions and design.

Additionally, multiple rectifier circuits were designed and tested on an AVA with four corrugated slots. The rectifier circuit plays a crucial role in converting the RF signal received by the antenna into a DC signal. To enhance RF-to-DC conversion efficiency, a multi-stage voltage multiplier topology was implemented, as shown in Fig. 2. This layered

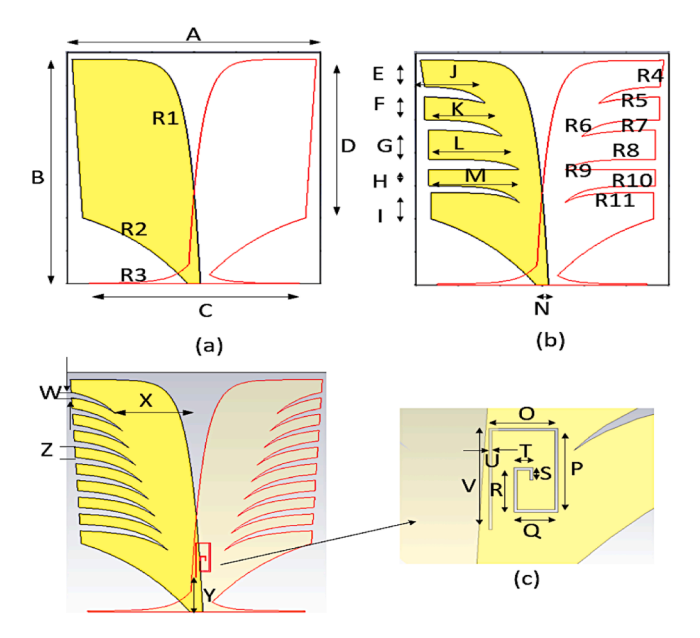


Fig. 1. Antipodal Vivaldi Antenna (AVA) (a) The front view of the AVA, showing the main tapered slot and patch design, (b) Illustration of the applied corrugation structures on the patch, which enhance antenna performance by improving impedance matching and directivity, and (c) A detailed view of the Rectangular Spiral Slot (RSS) integration, which is used for band rejection and frequency tuning.

Table 1Dimension of the Antenna (see on Fig. 1).

Par	Dim (mm)	Par	Dim (mm)	Par	Dim (mm)
A	60	R	0.35	0	3.5
В	70	R1	0.05	P	8.5
C	25	R2	0.05	Q	2.5
D	26.5	R3	0.25	R	4.5
E	8	R4	0.25	S	1.25
F	7	R5	0.15	T	1.5
G	9	R6	0.25	U	0.25
Н	5	R7	0.15	V	10.25
I	8	R8	0.25	W	1.6
J	14.5	R9	0.25	X	18.5
K	18.5	R10	0.25	Y	10
L	21.5	R11	0.25	Z	3
M	21	N	3		

rectifier circuit increases the output voltage derived from the input RF voltage, which is essential for RF energy harvesting, as ambient RF signals are often weak and variable. The rectifier design employs a multi-stage configuration using a combination of diodes and capacitors to double the output voltage, as illustrated in Fig. 2. The RF-to-DC conversion efficiency can be expressed as follows [29,30]. The rectifier circuit uses a Villard voltage multiplier topology, where the diode acts as a multi-stage rectifier and the capacitor acts as a coupling and storage device. Power Conversion Efficiency (PCE) is a key parameter in evaluating the performance of a rectenna system, indicating the extent to which received radio frequency (RF) power can be converted into direct current (DC) power. Mathematically, PCE is expressed by the Eq. (2) and (3):

$$\eta_{RF-DC} = \frac{P_{DC}}{P_{RF}} = \frac{V_{DC} \times I_{DC}}{P_{RF}} = \frac{V_{DC}^2}{P_{RF} \times R_L}$$
(2)

$$P_{DC}(W) = 10 \frac{P_{DC}(dBm) - 30}{10} \tag{3}$$

where η_{RF-DC} is the power conversion efficiency, V_{DC} is the DC output voltage generated by the rectifier circuit, P_{RF} is the RF input power received at the rectifier input terminal, and R_L is the load resistance connected to the rectifier output. The V_{DC} value can be obtained directly through measurement using a multimeter or oscilloscope with a DC probe, while R_L is the resistance value intentionally selected in the experimental design, typically determined based on output power optimization. Meanwhile, P_{RF} can be determined either through direct measurement using an RF power meter or theoretically using wave propagation equations. To determine the input rectenna Rf, it can be calculated using Friis equation. Theoretical calculations of RF input power often refer to the free-space path loss equation, which in logarithmic form is written as Eq. (4):

$$Pr = Pt + Gt + Gr - Lp (4)$$

Pt is the transmitter power obtained from the transmitter device specifications or RF measuring equipment, Gt is the transmitter antenna gain, and Gr is the receiver antenna gain (rectenna), both of which are obtained from the datasheet or electromagnetic simulation results using software such as CST or HFSS. As for Lp, which is path loss, it is calculated using the Eq. (5)

$$L_P = 20\log_{10}(d) + 20\log_{10}(f) + 147.55 \tag{5}$$

Where d is the distance between the transmitter and receiver in meters, which can be physically measured in a laboratory, and f is the system operating frequency in MHz, corresponding to the RF source used. By carefully combining all these parameters, one can accurately estimate the efficiency of the rectenna system and understand the influence of each variable in the power conversion chain from RF to DC. Where Lp is the constant value of Free Space Path Loss (FSPL) of 147.55 dB. Mea-

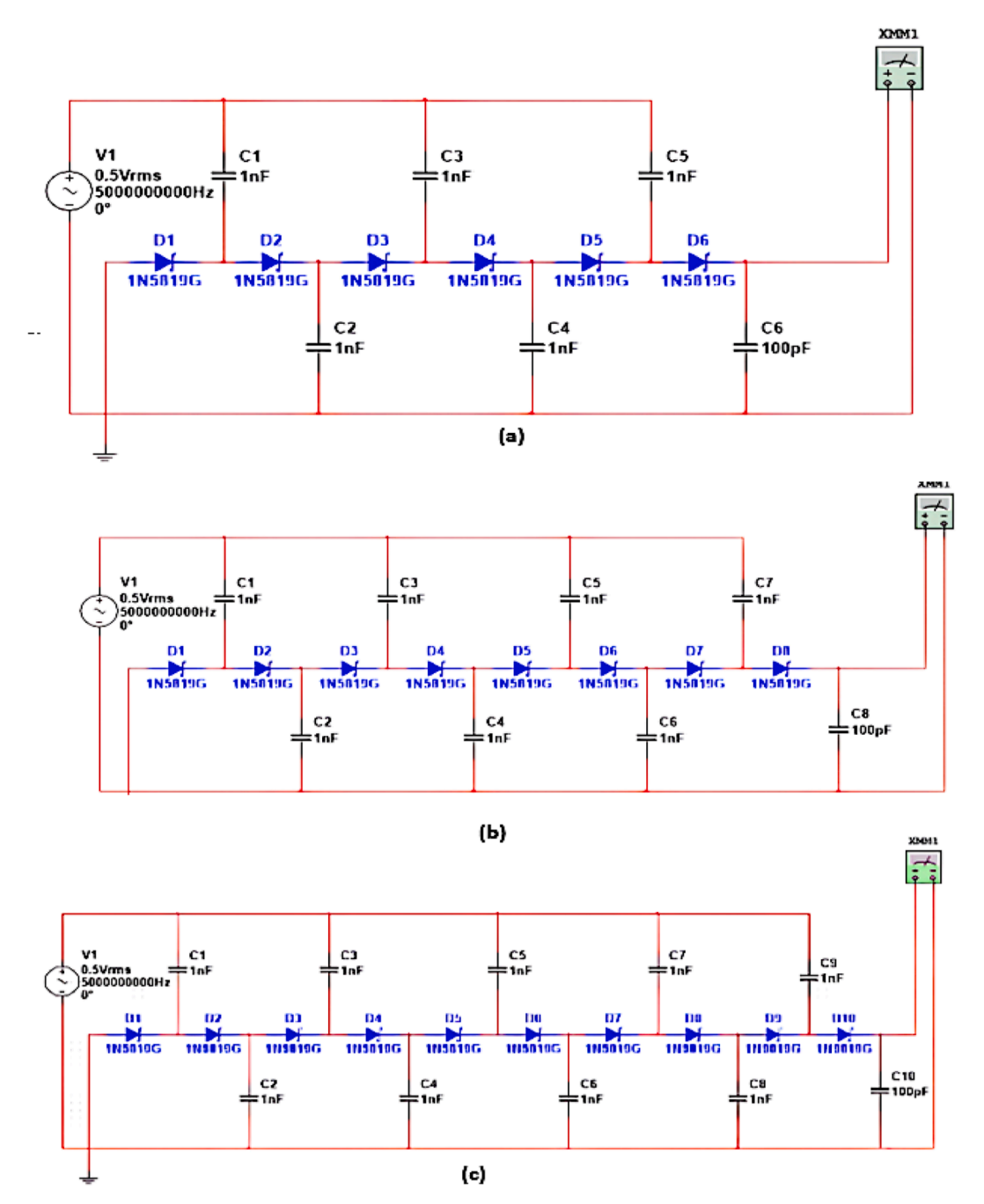


Fig. 2. Rectifier design: (a) three-stage, (b) four-stage, and (c) five-stage configurations.

surements were taken assuming no signal obstructions.

The 1N5819 diode is a type of Schottky diode that is widely used in high-frequency rectifier applications such as rectennas, due to its superior characteristics in terms of switching speed and low forward voltage. According to the datasheets from ON Semiconductor, Vishay, and STMicroelectronics, this diode has a number of important specifications that make it highly suitable for RF-DC conversion.

Technically, the 1N5819 has a typical forward voltage drop (V_f) of only about 0.3 to 0.45 V at a current of 1 A, which is significantly lower than that of a standard silicon diode (approximately 0.7 V). This low voltage is crucial in rectenna systems, especially when handling very low-power RF signals (such as -10 dBm to 0 dBm), as it allows more RF energy to be converted into DC voltage without being "lost" at the diode junction. This diode also features fast switching capability with a junction capacitance (Cj) of only approximately 110 pF, as well as extremely

short reverse recovery time, making it highly responsive to high-frequency signals, such as those in the 900 MHz to 2.4 GHz band.PDC represents the power output, PRF is the RF power input, VDC is the output voltage, IDC is the DC input, and RL is the load resistance. The overall conversion efficiency of electromagnetic radiation to DC, also known as radiation-to-DC efficiency, is used to evaluate the effectiveness of the rectenna system. This efficiency is a combination of radiation-to-AC efficiency, which primarily depends on the antenna, and AC-to-DC conversion efficiency, which is mainly determined by the rectification circuit [38].

3. Result and discussion

Fig. 3 illustrates the differences in directivity and reflection coefficient between an AVA without corrugation, an AVA with a single

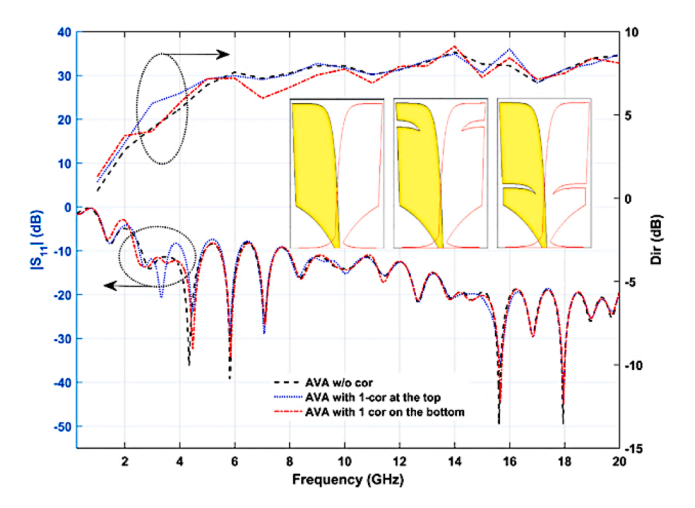


Fig. 3. S_{11} and Directivity performance between AVA without corrugation and AVA with 1- corrugation slot.

corrugation on the top radiator, and an AVA with a single corrugation on the bottom radiator. The figure shows that the reflection coefficient values across all frequencies from 2.3 to 20 GHz vary only slightly. The performance of reflection coefficient at $-10~\mathrm{dB}$ at low-end frequencies is obtained at 2.38 GHz, 2.52 GHz, and 2.6 GHz for AVA with one bottom corrugation, one top corrugation, and without corrugation structure, respectively. In addition, there is a slight difference in the directivity of the three AVA models. At 3 GHz, the AVA with one top corrugation has a directivity of 5.71 dBi, while the AVA with one bottom corrugation has a directivity of 4.05 dBi and the one without corrugation structure has a directivity of 4.24 dBi. However, the antenna with one corrugation on top and one without corrugation structure has a higher directivity at 7 GHz than the AVA with one corrugation on the bottom. The difference in directivity and reflection coefficient for the single corrugation antenna is not very significant.

Fig. 4 compares the directivity and reflection coefficient of antennas without corrugation to those with two corrugations at different locations. It is evident that at the low-end frequency, the first resonance at $-10~\rm dB$ reach for AVA with two corrugated antennas at 2.32 GHz. The AVA with corrugated below the antenna forms the first resonance at $-10~\rm dB$ at 2.27 GHz, while AVA without corrugation at the 2.6 GHz frequency. This indicates a boost in bandwidth performance of approximately 330 MHz at the low end of the frequency.

The AVA with the two corrugated sections below has a directivity of

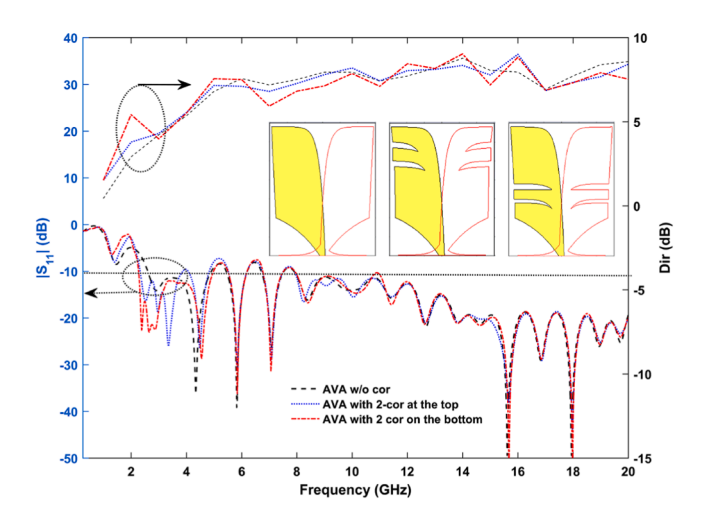


Fig. 4. S11 and Directivity performance between AVA without corrugation and AVA with 1- corrugation slot.

5.42 dBi at the 2 GHz frequency, whereas the AVA with the corrugated sections above has a directivity of 3.79 dBi, and the AVA without the corrugation has a directivity of 2.91 dBi. The directivity between AVA with two corrugated places below and AVA without corrugation is thus increased by 2.51 dBi at the 2 GHz frequency, according to these simulations

Fig. 5 compares the directivity and reflection coefficient of AVA without corrugation and with 1, 2, 3 and 4 corrugations on the top of the antenna. At frequencies lower than 5 GHz, the disparity in S_{11} performance is very apparent. AVA without corrugation has a low-end resonance frequency of S_{11} (-10 dB) at 2.6 GHz with a minimum impedance at -36.27 dB at 4.3 GHz. AVA with three corrugations has an S_{11} at -10 dB at frequency of 2.25 GHz and results a minimum S_{11} below 5 GHz of -40.64 dB at 3.2 GHz. There are multiple resonance frequencies below 5 GHz for AVA with four corrugations, with a minimum S_{11} of -51.64 dB at 2.58 GHz. That antenna has S_{11} of the antenna is nearly all below -15 dB at the 2.29 GHz to 3.43 GHz.

Based on previous simulation results, it was discovered that the antenna with four corrugations had the best performance in terms of return loss. It is beneficial to state an antenna as an equivalent circuit because it allows for the antenna to be treated in the same manner as other components. This allows for additional analysis to be carried out using traditional electric circuit theory and transmission line theory [39–41]. Fig. 6 illustrates the tuned RLC equivalent circuit of the proposed antenna, along with the reflection coefficient. The reflection coefficients produced by CST are compared with the reflection coefficients obtained using ADS, and both show agreement in shape, resonance frequency, and bandwidth as shown in Fig. 7.

Whereas Fig. 8 shows that at the 2 GHz frequency, the AVA with corrugation exhibits better directivity than the AVA without corrugation. AVA without corrugation has a directivity of 2.9 dBi at 2 GHz, however the AVA with three corrugations has a directivity of 5.73 dBi, which is 2.82 dBi higher than AVA without corrugation. But at 7 GHz, the converse is true, with 4 corrugations doing the worst out of all of them. The instability of increased directivity occurs at all frequencies. At lower frequencies, the corrugated structure has the potential to boost directivity; however, at higher frequencies, the directivity of the structure is rather variable. This occurs due to the fact that the antenna is constructed out of FR4 material, which means that there will be dielectric losses at high frequencies.

From the simulation results as shown in Fig. 9, it was found that there was a slight difference in the performance of the reflection coefficient between AVA types A, B and C. AVA type A has a minimum reflection coefficient at frequencies below 5 GHz of -51.65 dB at 2.58 GHz, AVA type B has the lowest reflection coefficient at -41.49 dB at the 2.76 GHz frequency, AVA Type-C has the lowest coefficient of -31.53 dB at the 3.11 GHz frequency.

However, AVA type-C also had a resonance at 1.98 GHz of −19.26 and had the lowest return loss at the 16.8 GHz frequency of −58.081 dB. The difference in the number of slots on corrugated can affect return loss performance, especially at low frequencies. From the directivity simulation results, it was found that AVA type C directivity is the best at most frequencies below 12 GHz. At the 2 GHz frequency, AVA type-C has a directivity of 8.03 dB, while AVA type-A has a directivity of 5.69 dBi and AVA B of 4.98 dBi. This means there is an increase of 3.05 dBi between AVA Type C and B at the 2 GHz frequency. Meanwhile, from the simulation results it was found that AVA type C has the highest directivity at the 15 GHz frequency of 9.07 dBi. It is possible to get a higher level of directivity by constructing a corrugated structure that has a greater number of slots, a narrower slot width, and deeper exponential slots (close to the two tapered slots in the middle). However, at a frequency of around 2 GHz, it is seen that in terms of reflection coefficient performance, a smaller number of corrugations has better performance than a large number of corrugated.

Figs. 10 shows the difference in return loss performance of AVA types C with the rectangular spiral strip slot structure on the opposite side of

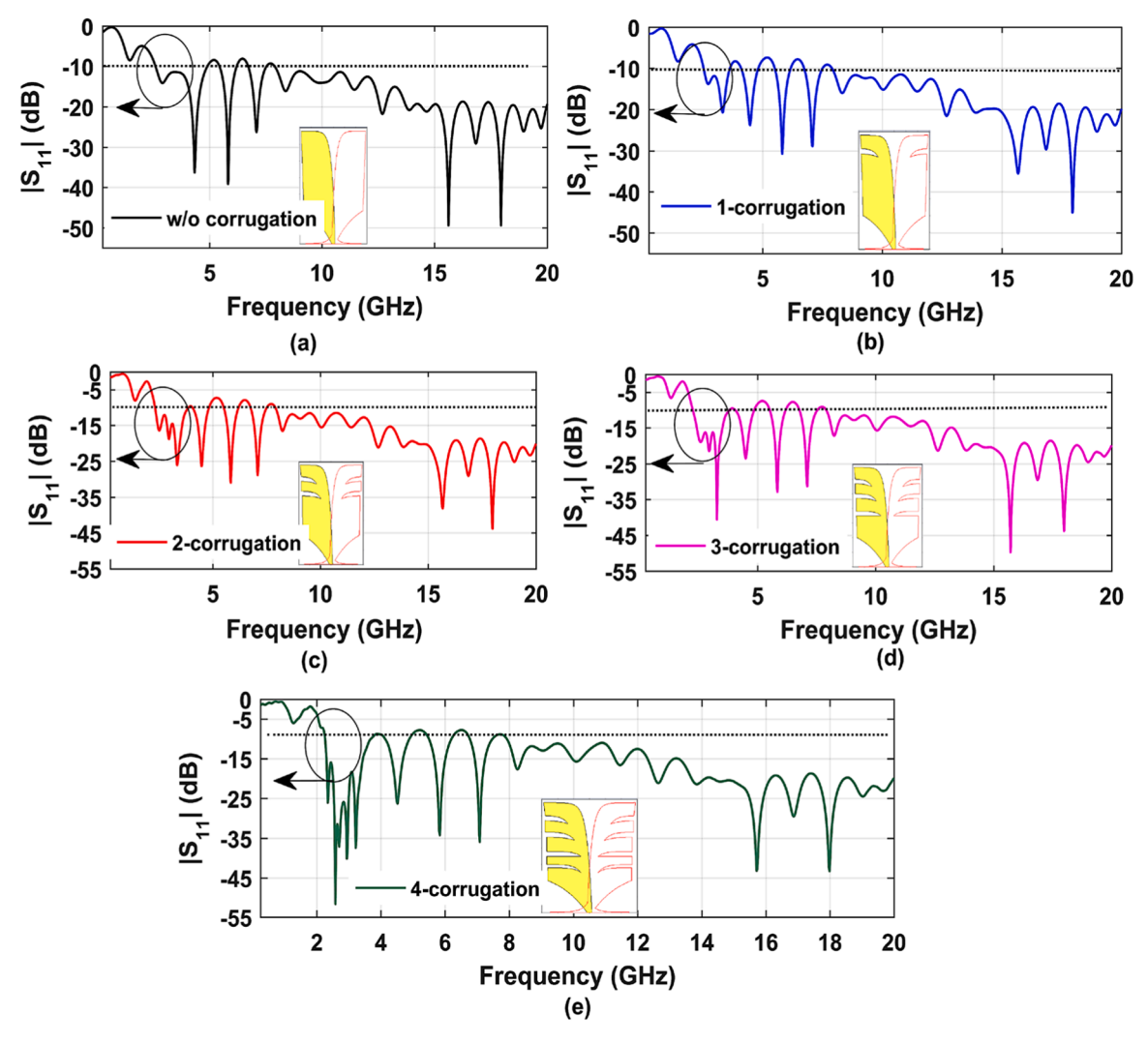


Fig. 5. Simulated |S₁₁| (dB) versus frequency (GHz) for different numbers of corrugations:
(a) Without corrugation, (b) With 1-corrugation, (c) With 2-corrugations, (d) With 3-corrugations, and (e) With 4-corrugations.

the feeder and located quite close to the feeding. From the simulation results, it can be seen that the return loss value forms a notched frequency band by changing the length of ys. In Fig. 10 it can be seen that when ys = 3.75 mm the notched band occurs at 3.24 to 3.91 GHz, while when ys = 6.25 mm the notched frequency band occurs at 3.03 to 3.65 GHz, when ys = 8.75 mm the notched band occurs at a frequency of 2.72 up to 3.29 GHz and when ys = 11.25 mm, the band is notched frequency occurs at 1.39 to 1.94 GHz, also at 2.57 to 2.94 GHz. It can be concluded that, the longer ys is, the more the notched frequency band shifts to the lower frequency or shifts to the left. The use of a RSS structure can be used to filter the desired frequency by adjusting the length and geometry of the spiral as well as the position of the spiral.

Fig. 11 shows a comparison of the polar radiation pattern of the AVA antenna without corrugation and the AVA radiation pattern with 4 corrugations at theta 90° at frequencies 2 GHz, 4 GHz and 7 GHz. At the 2 GHz and 4 GHz frequencies, the radiation pattern of AVA with 4 corrugations has a higher main lobe than AVA without corrugations. At the 2 GHz frequency AVA without corrugation produces a Main lobe of 2.9 dBi, main lobe direction 170 deg, angular width 3 dB, 74.6 deg and Side lobe level –1.4 dB while AVA with 4 corrugations produces 5.73 dBi, main lobe direction 87 deg, Angular width 3 dB 67 deg and Side lobe level of 0.8 dB. At the 2 GHz frequency, it can be seen that there is an increase in the main lobe of 2.83 dBi. At 4 GHz, AVA without corrugation produces main lobe 5.35 dBi, main lobe direction 124 deg,

angular width 105.9 deg and side lobe level -4.2 dB while for AVA with 4 corrugations produces main lobe 6.93 dB, main lobe direction 92 deg, angular width 80.2 deg and Side lobe level -11.1 dB. At the 4 GHz frequency, AVA with corrugation produces a main lobe increase of 1.58 dBi and an increase in side lobe level performance of 6.9 dB. At the 7 GHz frequency, AVA without corrugation produces 7.22 dB while AVA with 4 corrugations produces 6.92 dB main lobe. At the 7 GHz frequency the AVA main lobe without corrugation is higher than the main lobe with corrugation. The provision of a corrugation structure can improve the performance of radiation patterns at several working frequencies, especially at frequencies below 5 GHz. So that corrugation structures can be used as an alternative to improve the performance of radiation patterns at the desired frequencies.

The co-polarization and cross-polarization of the AVA antenna with four corrugations are depicted in Fig. 12. The radiation pattern of co-polarization is established at Theta = 90 degrees, whereas the cross-polarization is defined at Phi = 0 degrees. At a frequency of 2 GHz, the co-polarized antenna generates a main lobe magnitude of 5.13 dBi, positioned at 88 degrees. At frequencies of 3 and 4 GHz, the co-polarized main lobe exhibits gains of 5.99 dBi and 7.14 dBi, respectively, with main lobe directions of 83 degrees and 94 degrees. At frequencies of 2, 3 and 4 GHz, the cross-polarization antenna exhibits main lobe gains of -3.84 dBi and -4.1 dBi, respectively, with corresponding main lobe angles of 276 degrees, 189 degrees, and 2 degrees. Fig. 12 illustrates a

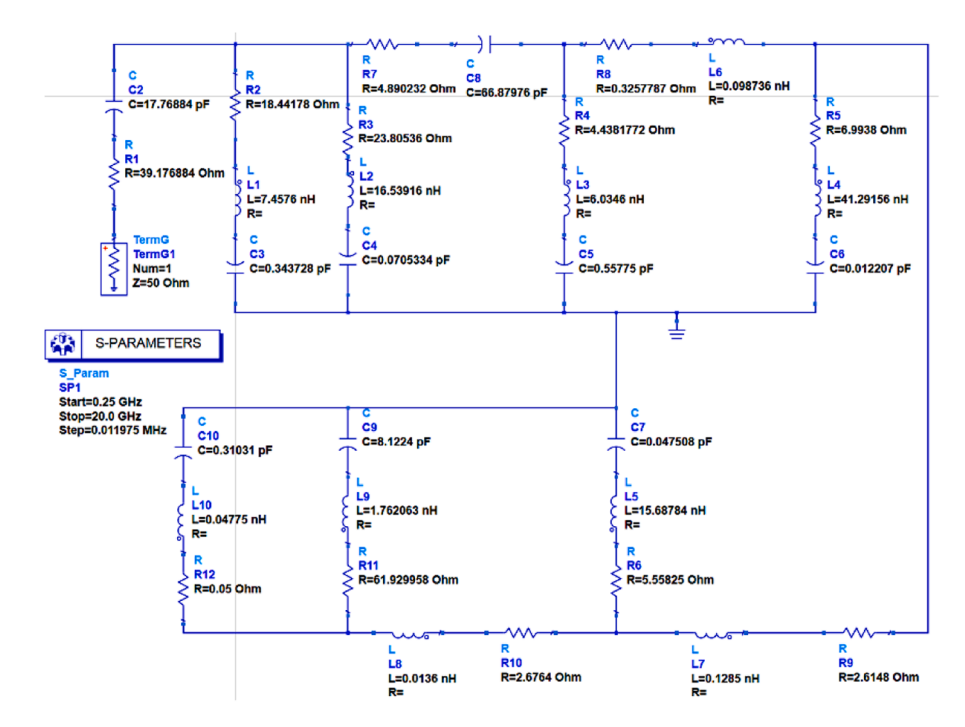


Fig. 6. RLC equivalent Circuit of the Corrugated Antipodal Vivaldi Antenna.

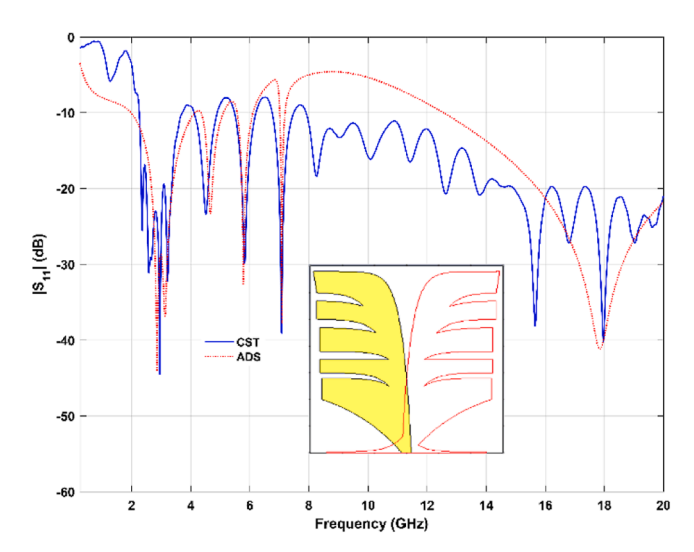
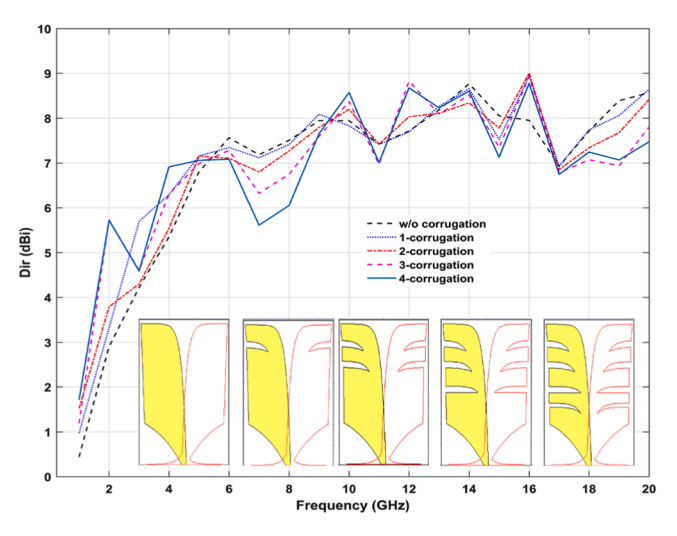


Fig. 7. validation simulation result of the proposed antenna between the CST circuit and the ADS circuit.

substantial disparity between Co and Cross polarization, indicating that the orientation of antenna polarization can be modified to optimize signal reception.

The surface current differential between AVA with and without corrugation at frequencies of 2 GHz and 4 GHz is depicted in Fig. 13. It is evident from the Figure that the area of the surface current antenna with corrugation that is highlighted in red has a higher concentration of corrugation.

In Fig. 14, the simulation and measurement results of the AVA antenna with four corrugations at frequencies ranging from 2 to 20 GHz are compared. In particular at frequencies lower than 10 GHz, there was a agreement between the modeling and measurement results. The reflection coefficient value that is obtained is only slightly different from the simulation result around the frequency range of 2 to 4 GHz; however, the measurement result at that frequency still reveals that the reflection coefficient value is lower than $-15\ \mathrm{dB}$ throughout the entire



 $\begin{tabular}{lll} {\bf Fig.} & {\bf 8.} & {\bf Directivity} & {\bf performance} & {\bf evaluation} & {\bf under} & {\bf different} & {\bf corrugation} \\ {\bf AVA} & {\bf cases}. \\ \end{tabular}$

frequency range. There is a tiny disparity between the simulation result and the measurement result for frequencies that are more than 10 GHz. This disparity can be attributed to a number of different factors inside the system. The cable specifications that are utilized for high frequencies might not be adequate, which would result in some loss caused by the cable. Additionally, the connector might also be responsible for some of the loss that results from the cable. On the other hand, this distinction is not really relevant.

In the meanwhile, measurements of the AVA antenna utilizing corrugation and a rectifier circuit are displayed in Fig. 15. Three different circumstances were used for the antenna tests using a succession of rectifiers. Measurements are made in open areas, enclosed areas, and on top of buildings. When measuring the rectenna in open space, the maximum voltage obtained on the circular antenna with a 5-stage rectifier circuit was 3.2 mV. When measuring the rectenna on top of the building, the maximum voltage obtained on the antenna with a 5-

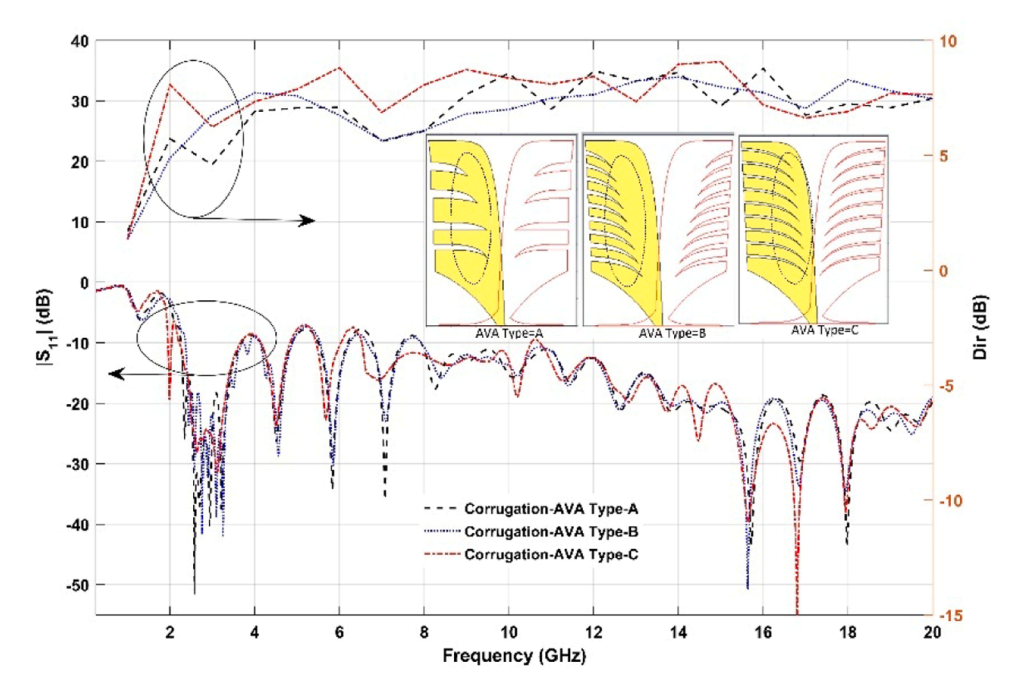


Fig. 9. S_{11} and Directivity performance of AVA type-A, AVA Type-B and AVA type-C.

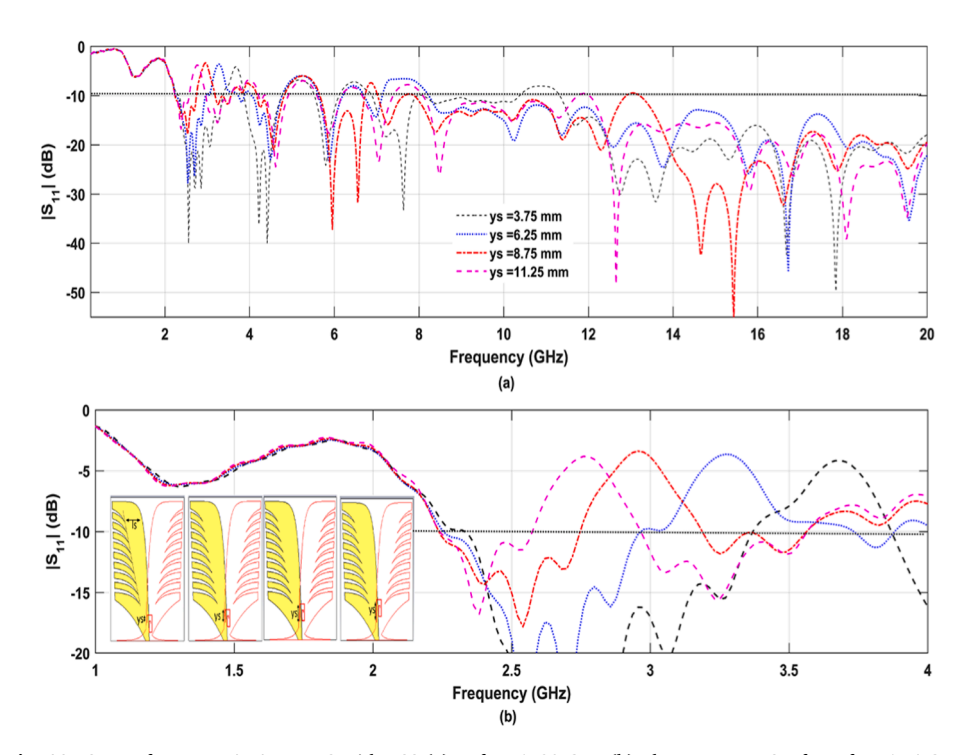


Fig. 10. S_{11} performance AVA Type C with RSS (a) at freq 1–20 GHz (b) The Zoom out S_{11} from freq 1-4 GHz.

stage rectifier circuit was 19.5 mV. And the lowest voltage was obtained on an antenna with a 3-stage rectifier circuit, namely 7.8 mV. Rectenna tests measured on top of a building produce more voltage than rectenna tests measured indoors. The antenna actually captures more electromagnetic wave signals when it is at a height, this can be because when it is at a height, the antenna can capture electromagnetic wave signals with minimal obstructions. Fig. 15(c) shows the rectenna measurements indoors with the influence of distance to the signal source from the router. The voltage performance obtained from the rectenna with the influence of distance is shown in Table 2 and it can be seen that the greater the distance to the router, the smaller the voltage produced, but

the higher the rectifier stage, the greater the voltage received.

The rectifier circuit was simulated using the Multisim simulator and has been directly measured in several different location conditions. From the voltage results obtained as shown in Fig. 15 and Table 2, the efficiency was calculated. In this study, the IN 5819 diode was used because it is cheaper and easier to obtain. The 1N5819 diode is a type of Schottky diode with low forward voltage and good peak forward current, so that in high-power RF input conditions or certain rectifier topologies it can increase the voltage at the junction. Several implementation studies show that the use of diodes in full bridge topologies or doubler circuits in practical designs such as prototype

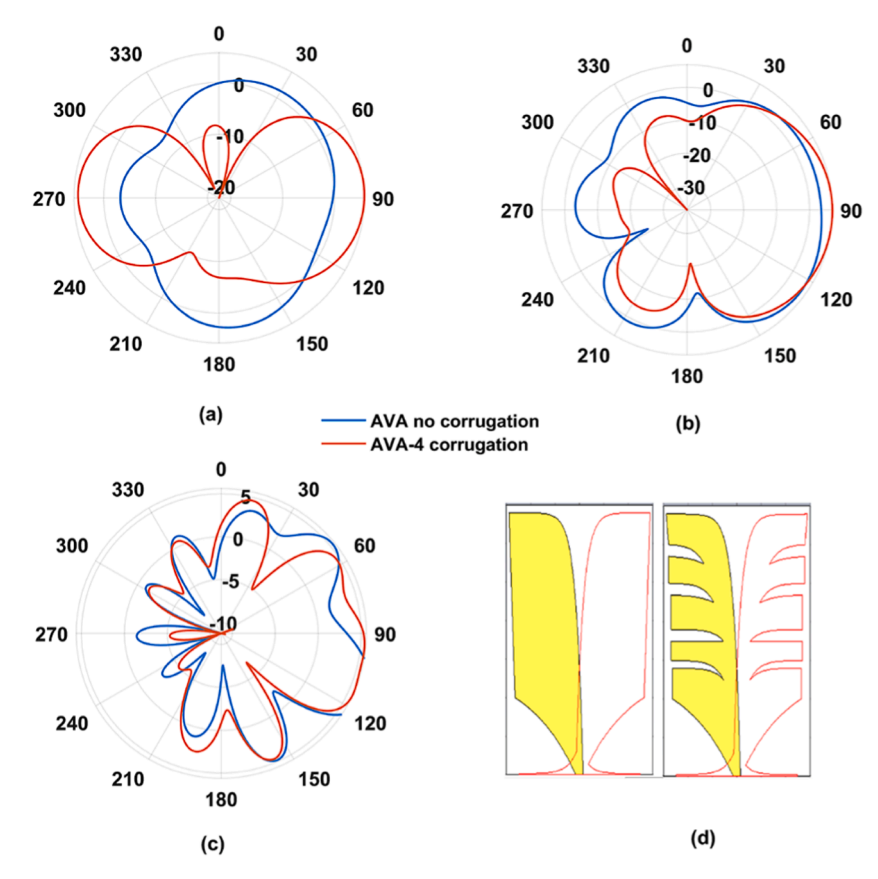


Fig. 11. Polar Radiation pattern performance at frequency (a) 2 GHz, (b) 4 GHz, (c) 7 GHz and (d) AVA w/o corrugation.

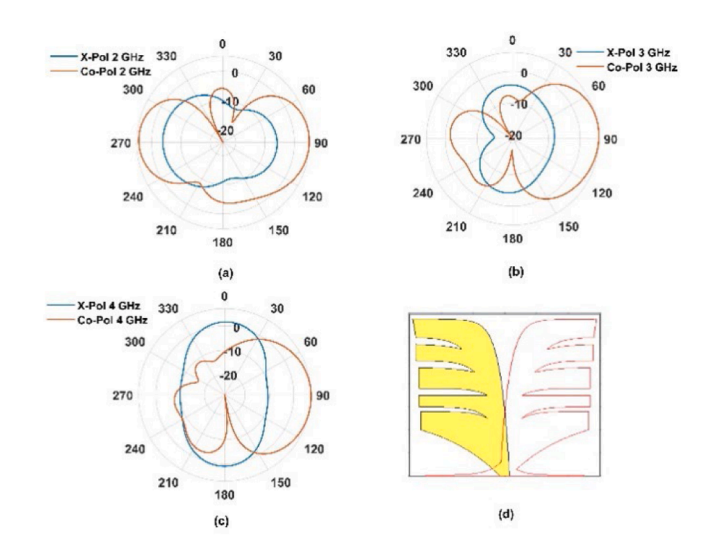


Fig. 12. Co and Cross Polarization of AVA With 4-corrugations. at frequency (a) 2 GHz, (b) 3 GHz, (c) 4 GHz and (d) AVA with 4 corrugation.

broadband rectifiers shows functional feasibility during testing. In the 1N5819 datasheet, the junction capacitance (Cj) has a large value. Where this effect can be overcome by matching techniques, the use of filters, or rectifier topologies such as Dickson or Villard type voltage-doublers that reduce the effect of input impedance at the working frequency [42–44]. The 1N5819 diode is very common, inexpensive, and available in many types, making it easier to prototype and apply multi-level power. The use of rectifier circuits with other topologies or other diode types may be possible to investigate in further research.

Table 3 shows a comparison of references related to the rectenna.

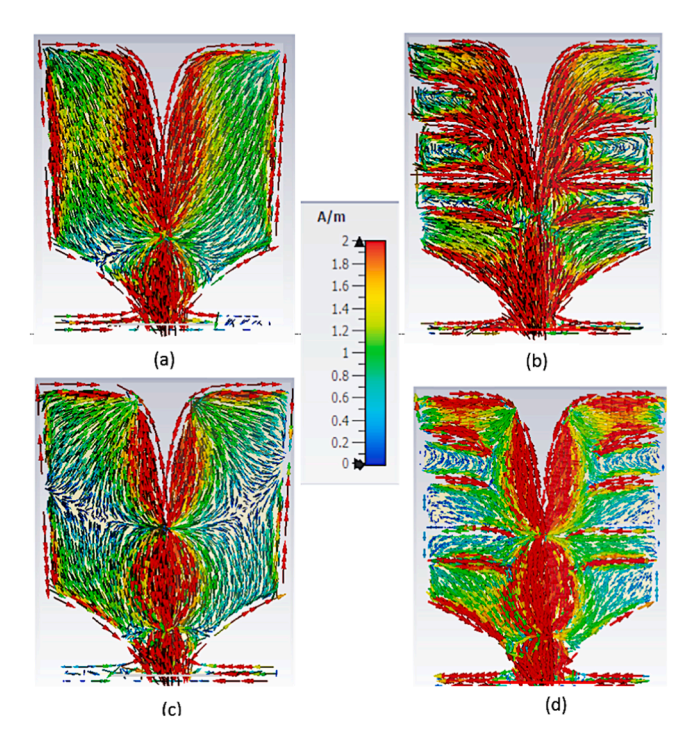


Fig. 13. Surface current AVA at frequency: (a) 2 GHz without Corrugation. (b) 2 GHz, 4-corrugation. (c) 4 GHz without Corrugation and. (d) 4 GHz, 4-Corrugation.

Some references show that the antenna only works in a bandwidth that is not too wide. In reference [22] the rectenna used is both a Vivaldi antenna, although it has a higher antenna directivity than the antenna

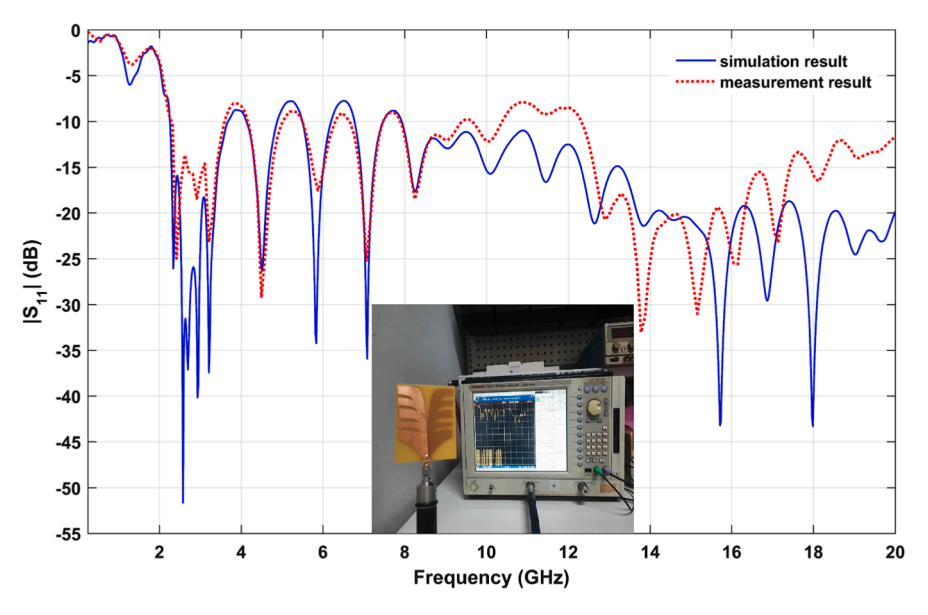


Fig. 14. Measurement and Simulation result of AVA with 4-Corrugation.

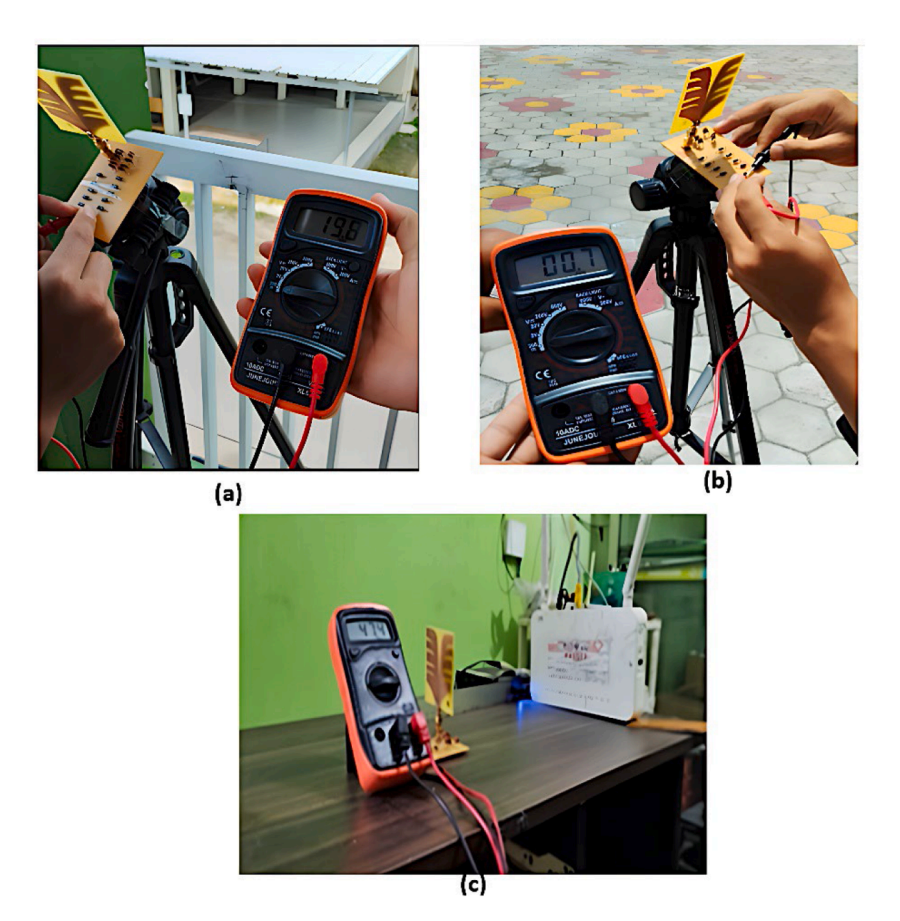


Fig. 15. Rectenna Measurement:(a) above the building, (b) Outdoor (under the building), and (c) Indoor (near router).

Table 2
Indoor Measurement result.

Distance from Router	Voltage 3-stages Rec	Voltage 4-stages Rec	Voltage 5-stages Rec
8 cm	18.1 mV	47.6 mV	900 mV
10 cm	17.1 mV	41.9 mV	800 mV
20 cm	10.6 mV	47.4 mV	0.100 mV

we made, but it only works at 2.4 and 5.8 GHz with a bandwidth that is not wide and has an efficiency that is not too high. A Vivaldi antenna, which operates in a broad frequency range of 2.2–12.1 GHz, is also used in Reference [45]. However, this antenna incorporates solar cells and has a lower bandwidth and maximum gain than the antenna we made. Additionally, it has a rectifier that only operates in the frequency range of about 2.4 GHz and generates a rectifier efficiency of 49 %. In reference [46] the antenna has a high gain of 12.7 dBi, but uses 6 layers of

Table 3Comparison of the purposed antennas in relation to relevant literature.

Ref	Freq (GHz)	Dir (dBi)	Antenna type	Dimension (mm)	Substrate type	Diode type	Efficiency
[8]	1.7 – 2.7	3	Rec Slot	55 × 55	Fr4	SMS 7630	40 %
[9]	0.9, 1.8	2.36	Monopole	50 × 50	FR4	HSMS 2850	70.1 %
[22]	2.4, 5.8	10.9, 10.2	CVA	150×210	FR4	Dickson 4	52.3 %
[26]	2.42	3.94	Microstrip	80×80	FR4	HSMS 2813	78.5 %
[27]	3.36 - 5.92	_	Dipole	41 × 35	FR4	HSMS 7630	42 %
[28]	2.45	8.1	Microstrip	70 × 64	Felt	HSMS 7630	73 %
[45]	2.2 - 12.1	5	CTSA	38×86	Polymer	HSMS 2850	49 %
[46]	5.8	12.7	FSS	91×52	Duroid	HSMS 7630	67.7 %
[47]	2.2	7.46	Octagonal	71×71	RT 5880	SMS 7621	50 %
[48]	1.6-2.65	3.53	Monopole	48×62	Duroid	HSMS 7630	42 %
[49]	0.45 - 0.9	3.5	Bowtie	160×160	FR4	HSMS 7630	77 %
[50]	1.85 - 6.85	6.82	Monopole	75×10	FR4	GVD	67.8 %
[51]	0.9, 1.8, 2.1	4.5	Monopole	100×87	RO 4003	SMS 7630	75 %
[52]	2.4	7.26	Microstrip	87×72	RT 5880	HSMS 2862	33 %
[53]	2-18	_	AVA	100.2×80.7	RO 4003	HSMS2860	72 %
[54]	5.8	7.6	Microstrip	49 × 34	RT 5880	SMS7621	77 %
Our Work	2.25-20	8.78	AVA	70×60	FR4	IN 5819	94.7 %

substrate with an FSS structure and uses a more complex port design and volume shaped antenna. Meanwhile, the single element antenna that we built has a bandwidth ranging from 2.25 to over 20 GHz, a more straightforward shape, a wider bandwidth, and more efficiency.

4. Conclusion

The study developed a compact Corrugated Antipodal Vivaldi Antenna (AVA) operating across a wideband frequency range from 2.3 GHz to over 20 GHz for energy harvesting applications. Parametric analysis was conducted to evaluate the impact of the number and position of corrugations on the antenna's reflection coefficients and radiation patterns. The results showed that AVAs with three or four corrugations exhibited higher directivity at 2 GHz (up to 5.73 dBi) compared to AVAs without corrugation (2.58 dBi). The corrugated structure also enhanced the reflection coefficient performance at lower frequencies. Additionally, the shape and placement of the rectangular spiral slot (RSS) structure were optimized to generate and control notched frequency bands. The AVA was integrated with rectifier circuits consisting of 2, 3, and 5 stages, enabling effective voltage reception for energy harvesting. Indoor tests using a router at various distances confirmed that the rectenna's energy harvesting performance improved with closer proximity to the router. The agreement between simulation and measurement data confirms that the proposed corrugated AVA is a strong candidate for wideband energy harvesting applications.

CRediT authorship contribution statement

Nurhayati Nurhayati: Writing – original draft, Supervision, Methodology, Conceptualization. Mohammad Iyo Agus Setyono: Software, Formal analysis. Ahmed J.A. Al-Gburi: Writing – review & editing, Validation, Project administration. Lilik Anifah: Resources, Investigation. Lusia Rakhmawati: Formal analysis, Data curation. Fitri Adi Iskandarianto: Visualization, Resources. Usman Ali: Software, Data curation.

Declaration of competing interest

The authors declare that they have no known competing financial interests or personal relationships that could have appeared to influence the work reported in this paper.

Acknowledgments

We are grateful to Universitas Negeri Surabaya for the funding provided under 321 Decree No. B/116175/UN38.III.1/LK.04.00/2024. The

authors are also grateful to Universiti Teknikal Malaysia Melaka (UTeM) for their support

Data availability

Data will be made available on request.

References

- Y. Mouzouna, et al., Design and fabrication of a miniature and compact tri-band antenna using CTSRR metamaterial and DGS methods for RFID and WiMAX applications, Int. J. Intell. Eng. Syst. 12 (2) (2019) 192–201.
- [2] A. Ali, M.E. Munir, M. Marey, H. Mostafa, Z. Zakaria, A.J.A. Al-Gburi, F.A. Bhatti, A compact MIMO multiband antenna for 5G/WLAN/WIFI-6 devices, Micromachines 14 (2023) 1153, https://doi.org/10.3390/mi14061153.
- [3] A.S. Taher, R.A. Fayadh, A.F. Humadi, Design of a patch antenna with three bands for vital signs monitoring devices, Int. J. Intell. Eng. Syst. 16 (4) (2023) 389–397.
- [4] Q.H. Kareem, M.J. Farhan, Compact dual-polarized eight-element antenna with high isolation For 5 G mobile terminal applications, Int. J. Intell. Eng. Syst. 14 (6) (2021) 187–197.
- [5] B.M. Ahmed, L.A. Abdul-Rahaim, Dual-podal of vivaldi vehicular antenna for IoV in 5G communications, Int. J. Intell. Eng. Syst. 17 (4) (2024) 1099–1107.
- [6] M. Fantuzzi, D. Masotti, A. Costanzo, A novel integrated UWB-UHF one-port antenna for localization and energy harvesting, IEEE Trans. Antennas Propag. 63 (9) (2015) 3839–3848.
- [7] A. Eid, J.G.D. Hester, J. Costantine, Y. Tawk, A.H. Ramadan, M.M. Tentzeris, A compact source-load agnostic flexible rectenna topology for IoT devices, IEEE Trans. Antennas Propag. 68 (4) (2020) 2621–2629.
- [8] S.S. Alja'afreh, C. Song, Y. Huang, L. Xing, Q. Xu, A dual-port, dual-polarized and wideband slot rectenna for ambient RF energy harvesting, in: 14th Eur. Conf. Antennas Propagation, EuCAP 2020, 2020, pp. 3–7.
- [9] S. Muhammad, J.J. Tiang, S.K. Wong, A. Smida, R. Ghayoula, A. Iqbal, A dual-band ambient energy harvesting rectenna design for wireless power communications, IEEE Access 9 (2021) 99944–99953.
- [10] Lalbabu Prasad, Harish Chandra Mohanta, Ahmed Jamal Abdullah Al-Gburi, Dual band rectenna for electromagnetic energy harvesting at 2.4 GHz and 5 GHz frequencies, Progr. Electromagn. Res. B 108 (2024) 75–88, https://doi.org/ 10.2528/PIERB24072102.
- [11] D.N. Elshaekh, H.A. Mohamed, H.A. Shawkey, S.I. Kayed, Printed circularly polarized spilt ring resonator monopole antenna for energy harvesting, Ain Shams Eng. J. 14 (6) (2023) 102182.
- [12] A.A.G. Amer, N. Othman, S.Z. Sapuan, A. Alphones, M.F. Hassan, A.J.A. Al-Gburi, Z. Zakaria, Dual-band, wide-angle, and high-capture efficiency metasurface for electromagnetic energy harvesting, Nanomaterials 13 (2023) 2015, https://doi. org/10.3390/nanol3132015.
- [13] A. Sabban, Novel meta-fractal wearable sensors and antennas for medical, communication, 5G, and IoT applications, Fractal Fract. 8 (2) (2024).
- [14] T.S. Almoneef, S.M. Saeed, M.A. Aldhaeebi, M.M. Bait-Suwailam, Wideband metasurface for microwave energy harvesting, in: 2019 IEEE Int. Symp. Antennas Propag. Usn. Radio Sci. Meet. APSURSI 2019 - Proc, 2019, pp. 1165–1166.
- [15] F. Yang, C. Song, Y. Hu, A high-gain wideband U-slot E-shaped patch antenna for on-body wireless energy harvesting applications, in: 2024 4th URSI Atl. Radio Sci. Meet. AT-RASC 2024, 2024, pp. 1–4.
- [16] K. Nadali, P. McEvoy, M.J. Ammann, A broadband circularly polarised slot antenna for ambient RF energy harvesting applications, in: 2022 Int. Work. Antenna Technol. iWAT 2022, 2022, pp. 153–156.

- [17] H. Saghlatoon, T. Bjorninen, L. Sydanheimo, M.M. Tentzeris, L. Ukkonen, Inkjet-printed wideband planar monopole antenna on cardboard for RF energy-harvesting applications, IEEE Antennas. Wirel. Propag. Lett. 14 (2015) 325–328.
- [18] Y. Zhang, A.K. Brown, Bunny ear combline antennas for compact wide-band dualpolarized aperture array, IEEE Trans. Antennas. Propag. (2011).
- [19] M. Abbak, M.N. Akıncı, M.Ç. Ayören, I. Akduman, Experimental microwave imaging with a novel corrugated vivaldi antenna, IEEE Trans. Antennas Propag. 65 (2017) 3302–3307.
- [20] P. Nijhawan, A. Kumar, Y. Dwivedi, A flexible corrugated vivaldi antenna for radar and see-through wall applications, in: 2018 3rd Int. Conf. Microw. Photonics, ICMAP 2018 2018-Janua, 2018, pp. 1–2.
- [21] N. Nurhayati, E. Setijadi, A.M. De Oliveira, D. Kurniawan, M.N. Mohd, Design of 1 × 2 MIMO palm tree coplanar vivaldi antenna in the e-plane with different patch structure, Electron 12 (2022) 1–23.
- [22] S. Li, F. Ghannouchi, R. Vyas, A dual-band rectenna with improved RF-DC sensitivity for wireless energy harvesting, in: 2019 IEEE Int. Symp. Antennas Propag. Usn. Radio Sci. Meet. APSURSI 2019 - Proc, 2019, pp. 1173–1174.
- [23] X. Zhang, C. Cao, C. Song, A Compact Dual-band, Dual-CP polarization wideband rectenna using reverse wilkinson power divider for wireless information and power transfer, IEEE Antennas Wirel. Propag. Lett. 23 (9) (2024) 2728–2732.
- [24] H. Mahfoudi, M. Tellache, H. Takhedmit, A wideband fractal rectana for energy harvesting applications, in: 2016 10th Eur. Conf. Antennas Propagation, EuCAP 2016, 2016, pp. 32–35.
- [25] A.Y. Iliyasu, M.R. Hamid, M.K.A. Rahim, M.F. Mohd Yusoff, M. Aminu-Baba, M. M. Gajibo, Wideband frequency reconfigurable metamaterial antenna design with double h slots, Bull. Electr. Eng. Inform. 9 (5) (2020) 1971–1978.
- [26] R. Pandey, A.K. Shankhwar, A. Singh, Design and analysis of rectenna At 2.42 Ghz for Wi-Fi energy harvesting, Prog. Electromagn. Res. C 117 (December) (2021) 89–98.
- [27] C. Guo, W. Zhang, A wideband CP dipole rectenna for RF energy harvesting, in: 2019 Cross Strait Quad-Regional Radio Sci. Wirel. Technol. Conf. CSQRWC 2019 -Proc, 2019, pp. 1–3.
- [28] S.E. Adami, et al., A Flexible 2.45-GHz power harvesting wristband with net system output from -24.3 dBm of RF power, IEEE Trans. Microw. Theory Tech. 66 (1) (2018) 380–395.
- [29] J. Ribadeneira-Ramírez, J. Santamaria, P. Romero, M.A. Paguay, Radio frequency energy harvesting device at ISM band for low power IoT, Prog. Electromagn. Res. M 122 (September) (2023) 11–20.
- [30] M. Khodaei, H. Boutayeb, L. Talbi, A. Ghayekhloo, Dual-Band RF rectifier using stepped microstrip line matching network for IOT sensors application, Prog. Electromagn. Res. C 149 (October) (2024) 81–86.
- [31] N. Nurhayati, F.Y. Zulkifli, E. Setijadi, B.E. Sukoco, M.N.M. Yasin, A.M. De Oliveira, Bandwidth, gain improvement, and notched-band frequency of SWB wave coplanar vivaldi antenna using CSRR, IEEE Access. 12 (February) (2024) 16926–16938.
- [32] A.N.D.N. Fahmi, N. Nurhayati, A.M. De Oliveira, M. Rohman, Reconfigurable of palm tree vivaldi antenna using square ring resonator for cognitive radio applications, in: Proceeding - IEEE 9th Inf. Technol. Int. Semin. ITIS 2023, 2023, pp. 221–225.
- [33] N. Nurhayati, A.N.D.N. Fahmi, P. Puspitaningayu, O. Wiriawan, B. Raafi, Wearable wideband textile coplanar vivaldi antenna for medical and IoT application, Prog. Electromagn. Res. C 148 (August) (2024) 145–156.
- [34] T.S. Almoneef, F. Erkmen, M.A. Alotaibi, O.M. Ramahi, A new approach to microwave rectennas using tightly coupled antennas, IEEE Trans. Antennas Propag. 66 (4) (2018) 1714–1724.
- [35] E. Nasrabadi, P. Rezaei, A novel design of reconfigurable monopole antenna with switchable triple band-rejection for UWB applications, Int. J. Microw. Wirel. Technol. 8 (8) (2016) 1223–1229.
- [36] S. Shen, Y. Zhang, C.Y. Chiu, R. Murch, A Triple-band high-gain multibeam ambient rf energy harvesting system utilizing hybrid combining, IEEE Trans. Ind. Electron. 67 (11) (2020) 9215–9226.
- [37] A. Eid, et al., A flexible compact rectenna for 2.40Hz ISM energy harvesting applications, in: 2018 IEEE Antennas Propag. Soc. Int. Symp. Usn. Natl. Radio Sci. Meet. APSURSI 2018 - Proc, 2018, pp. 1887–1888.
- [38] S. Chandravanshi, K.K. Katare, M.J. Akhtar, A flexible dual-band rectenna with full azimuth coverage, IEEE Access. 9 (2021) 27476–27484.
- [39] A. Arora, S. Singh, M.Varshney Vandana, M.K. Pandey, S. Pandey, A novel lotus shaped multiband patch antenna with improved performance, Prog. Electromagn. Res. Symp. 2019-June (2019) 3571–3577.
- [40] A. Varshney, D.N. Gencoglan, I. Elfergani, J. Rodriguez, C. Zebiri, T.M. Neebha, Characterizations of effective parameters and circuit modeling of U-coupled hybrid ring resonator band pass filter, IEEE Acces. 13 (November 2024) (2025) 2529–2545.
- [41] A. Varshney, V. Sharma, A comparative study of microwave rectangular waveguide-to-microstrip line transition for millimeterwave, wireless communications and radar applications, Microw. Rev. 26 (2) (2020) 26–37.
- [42] S. Hemour, C.H.P. Lorentz, K. Wu, Design of a highly efficient wideband multifrequency ambient RF energy harvester, Sensors (2016) 1–12.
- [43] L. Prashad, H.C. Mohanta, H.G. Mohamed, A compact circular rectenna for RF-energy harvesting at ISM band, Micromachines 14 (4) (2023) 1–14.
- [44] S. El Mattar, A. Baghdad, S. Said, E. Baghaz, Dickson voltage multiplier with 1 to 6 stages for dual-band rectifiers (2.45/5.8 GHz) with low input power, Telkomnika (Telecommunic. Comput. Electron. Control. 21 (4) (2023) 909–916.
- [45] T. Peter, T.A. Rahman, S.W. Cheung, R. Nilavalan, H.F. Abutarboush, A. Vilches, A novel transparent UWB antenna for photovoltaic solar panel integration and RF energy harvesting, IEEE Trans. Antennas Propag. 62 (4) (2014) 1844–1853.

- [46] M.C. Derbal, M. Nedil, High-gain circularly polarized antenna array for full incident angle coverage in rf energy harvesting, IEEE Acc. 11 (February) (2023) 28199–28207.
- [47] T.S. Almoneef, Design of a rectenna array without a matching network, IEEE Access 8 (2020) 109071–109079.
- [48] K. Çelik, E. Kurt, Design and implementation of a dual band bioinspired leaf rectenna for RF energy harvesting applications, Int. J. RF Microw. Comput. Eng. 31 (11) (2021) 1–16.
- [49] C. Song, Y. Huang, J. Zhou, P. Carter, Improved ultrawideband rectennas using hybrid resistance compression technique, IEEE Trans. Antennas Propag. 65 (4) (2017) 2057–2062.
- [50] B.R. Behera, P.R. Meher, S.K. Mishra, Metasurface superstrate inspired printed monopole antenna for rf energy harvesting application, Prog. Electromagn. Res. C 110 (February) (2021) 119–133.
- [51] M.T. Le, Q.C. Tran, A.T. Le, D. Minh, A multidirectional triple-band rectenna for outdoor rf energy harvesting from gsm900/gsm1800/umts2100 toward selfpowered iot devices, Prog. Electromagn. Res. M 104 (July) (2021) 1–12.
- [52] F. Zanon, U. Resende, G. Brandão, I. Soares, Energy harvesting system using rectenna applied to wireless powered remote temperature sensing, Prog. Electromagn. Res. C 114 (2021) 203–216.
- [53] M. Nosrati, P. Rezaei, M. Danaie, J. Khalilpour, A broadband integrated rectenna for microwave radio energy harvesting using an integrated hybrid sandwich power divider, e-Prime - Adv. Electr. Eng. Electron. Energy 11 (December 2024) (2025) 100891.
- [54] M. Nosrati, P. Rezaei, Efficient integrated 5 x 2 rectenna array for low RF energy recovery, AEU - Int. J. Electron. Commun. 161 (November 2022) (2023) 154547.



Nurhayati obtained the B.E., M.E., and D.E. degrees from Institut Teknologi Sepuluh Nopember (ITS) in Surabaya, Indonesia, as well as the master's and Ph.D. degrees in tele-communication multimedia from the Department of Electrical Engineering, Faculty of Electrical Technology, ITS. She is presently a Lecturer in the Department of Electrical Engineering, Faculty of Engineering, Universitas Negeri Surabaya. She serves as a Secretary at the Research Center, Institute for Research and Community Service, Universitas Negeri Surabaya. Her research interests encompass planar antennas, Vivaldi antennas, monopole antennas, wideband antennas, array antennas, radar antennas, and MIMO antennas.



Mohammad Iyo Agus Setyono received his bachelor's degree in electrical engineering education from Surabaya State University in 2010. He focused on the scientific fields of electronics and telecommunications. He is pursuing a Master's degree in Electronics Engineering with a concentration in Telecommunications and Smart Networks at Surabaya State University in 2023–2025. He works as a Vocational Teacher of Electronics Engineering. His research interests include electromagnetic applications, intelligent telecommunications, rectenna analysis and design, and wireless sensor networks.



Ahmed Jamal Abdullah Al-Gburi (Senior Member, IEEE) received his M.Eng. and Ph.D. degrees in electronics and computer engineering (telecommunication systems) from Universiti Teknikal Malaysia Melaka (UTeM), Malaysia, in 2017 and 2021, respectively. From December 2021 to March 2023, he was a Postdoctoral Fellow with the Microwave Research Group (MRG) at UTeM. He is currently a Senior Lecturer with the Faculty of Electrical and Electronic Engineering Technology (FTKEE) at UTeM. He has authored and coauthored numerous papers in journals and conference proceedings. His research interests include microwave sensors, metasurfaces, UWB antennas, array antennas, and miniaturized antennas for UWB and 5 G applications. He is a member of

the Board of Engineers Malaysia (BEM) and the International Association of Engineers (IAENG). He has received the Best Paper Award from the IEEE community and has earned several gold, silver, and bronze medals in international and local competitions. In 2023 and 2024, he was recognized as one of the top 2 % of scientists worldwide by Stanford University, as published by Elsevier.



Lilik Anifah was born in Gresik, East Java, Indonesia, in 1979. He obtained a B.S. in Engineering Physics and both an M.S. and a Doctorate in Electrical Engineering from Institut Teknologi 10 Nopember Surabaya, Indonesia, in 2007 and 2013, respectively. Since 2003, she has been a lecturer in Electrical Engineering at the Faculty of Engineering, Universitas Negeri Surabaya, Indonesia. Her research interests encompass intelligence pattern recognition, applications of artificial intelligence, image processing, and intelligent systems.



Fitri Adi Iskandarianto obtained a B.S. in Engineering Physics and an M.S. from Institut Teknologi 10 Nopember Surabaya, Indonesia. Since 2006, she has been a lecturer in Instrumentation Engineering at the Faculty of Vocational, Institut Teknologi Sepuluh Nopember, Indonesia. His research interests encompass Metrology, Instrumentation, Automation, Process Control and Conversion Energy.



Lusia Rakhmawati graduated with a doctoral degree from ITS in 2020 in the field of multimedia communications. His current research is about image processing, security communication, telecommunications signals, communication systems, and virtual laboratories. Now he serves as coordinator of the UNESA electrical engineering undergraduate study program.



Usman Ali obtained his B.Sc., M.Sc., and Ph.D. degrees in telecommunication engineering from the University of Engineering and Technology (UET), Peshawar, Pakistan, in 2012, 2017, and 2023, respectively. He is presently a Lecturer in the Department of Telecommunication Engineering at UET Mardan, Pakistan. His research interests encompass wearable antennas, synthetic aperture radar (SAR) analysis, implantable antennas, 5 G antennas, millimeter-wave antennas, reconfigurable antennas, metamaterials, metasurfaces, and electromagnetic bandgap structures.